HHS Public Access

Author manuscript

J Neuropathol Exp Neurol. Author manuscript; available in PMC 2016 June 01.

Published in final edited form as:

J Neuropathol Exp Neurol. 2015 June ; 74(6): 527–537. doi:10.1097/NEN.0000000000000197.

Abnormalities in the Tricarboxylic Acid Cycle in Huntington Disease and in a Huntington Disease Mouse Model

Nima N. Naseri, BS[a], **Hui Xu, BM**[a], **Joseph Bonica, BS**[a], **Jean Paul G. Vonsattel, MD**[b], **Etty P. Cortes, MD**[b], **Larry C. Park, PhD**[c], **Jamshid Arjomand, PhD**[c], and **Gary E. Gibson, PhD**[a]

[a]Weill Cornell Medical College, Brain Mind Research Institute, Burke Medical Research Institute, White Plains, New York

[b]New York Brain Bank, Taub Institute, Columbia University, New York, New York

[c]CHDI Management/CHDI Foundation, Inc., Los Angeles, California

Abstract

Glucose metabolism is reduced in the brains of patients with Huntington disease (HD). The mechanisms underlying this deficit, its link to the pathology of the disease and the vulnerability of the striatum in HD remain unknown. Abnormalities in some of the key mitochondrial enzymes involved in glucose metabolism, including the pyruvate dehydrogenase complex (PDHC) and the tricarboxylic acid (TCA) cycle, may contribute to these deficits. Here, activities for these enzymes and select protein levels were measured in human postmortem cortex and in striatum and cortex of an HD mouse model (Q175); mRNA levels encoding for these enzymes were also measured in the Q175 mouse cortex. The activities of PDHC and nearly all of the TCA cycle enzymes were dramatically lower (−50%–90%) in humans than in mice. The activity of succinate dehydrogenase increased with HD in human (35%) and mouse (23%) cortex. No other changes were detected in the HD cortex or mouse striatum. In Q175 cortex, there were increased activities of PDHC (+12%) and aconitase (+32%). Increased mRNA levels for succinyl thiokinase (+88%) and isocitrate dehydrogenase (+64%), suggested an upregulation of the TCA cycle. These patterns of change differ from those reported in other diseases, which may offer unique metabolic therapeutic opportunities for HD patients.

Keywords

Aconitase; Huntington disease; Mitochondrial dysfunction; Pyruvate dehydrogenase complex; Q175 knock-in mouse model; R6/2 transgenic mouse model; Succinate dehydrogenase; Tricarboxylic acid cycle

INTRODUCTION

Huntington disease (HD) is an autosomal dominant, late-onset neurodegenerative disease that impairs motor function and causes selective death of neurons in the brain. The striatum

Send correspondence to: Gary E. Gibson, Weill Cornell Medical College, Brain Mind Research Institute, Burke Medical Research Institute, 785 Mamaroneck Avenue, White Plains, NY 10605. Phone: 914-597-2291; ggibson@med.cornell.edu.

is particularly vulnerable (1). HD is caused by excessive polyglutamine (CAG) repeats in the huntingtin gene (*HTT*) (2). The factors that link the gene defects to the neurodegeneration and neurological manifestations are unknown. Although mutant Htt (mHtt) aggregates in the affected neurons, the role of these protein aggregates is poorly understood (3).

Altered glucose metabolism is widely implicated in several neurodegenerative disorders. 18-Fluoro-deoxyglucose positron emission tomography (i.e. FDG-PET) studies have shown that glucose metabolism is decreased in caudate putamen from HD brains (4–6). The current experiments tested the role of the mitochondrial tricarboxlyic acid (TCA) cycle in brains from the Q175 mouse model of HD and from patients who died with HD. The TCA cycle and the entry-level protein complex, pyruvate dehydrogenase complex (PDHC), provide the main pathway for generating reducing equivalents (e.g. NADH). The electron transport chain uses these reducing equivalents to produce ATP. Glucose is first converted to pyruvate, which then undergoes oxidative decarboxylation to form acetyl-CoA before ultimately generating reducing equivalents. Altered activities of complexes I-IV of the electron transport chain are well-documented in the caudate nucleus of HD brains but there are incomplete data for TCA cycle enzyme changes in several regions of the brain. Because NADPH, another reducing equivalent, is generated by the pentose shunt, the mRNA for transketolase, a key enzyme of the pentose shunt, was also measured.

The PDHC, the enzymes of the TCA cycle and their respective relevant coding genes are shown in order of the cycle (Fig. 1). Changes in all of the enzyme activities of the TCA cycle have been examined in schizophrenia (7), and Alzheimer disease (AD) (8), but never in HD. For example, in dorsal lateral prefrontal cortex from patients who died with AD, some enzyme activities (e.g. of PDHC and α-ketoglutarate dehydrogenase complex [KGDHC]) go down whereas others (e.g. succinate dehydrogenase [SDH] and malate dehydrogenase [MDH]) are increased compared to controls (8). In the dorsal lateral prefrontal cortex of patients with schizophrenia, activities of aconitase, KGDHC and succinyl thiokinase (STH) were lower than in controls, but SDH and MDH were higher than in controls (7). PDHC, citrate synthase (CS), isocitrate dehydrogenase (ICDH) and fumarase activities (as measured in the same study of schizophrenia brains) were unchanged. Some enzymes of the TCA cycle have been examined in HD in independent studies, but never collectively in the same study. Because the TCA cycle is highly integrated, measuring just one enzyme does not indicate the full impact of the disease on the TCA cycle or the impact of the changes on the disease process (9). PDHC (10), KGDHC (11), aconitase (12), CS (12), and SDH (13) activities have all been reported to be down in either human HD brains, R6/2 mice, or malonate/3-NP mouse models of HD compared to their respective controls.

In contrast to the transgenic R6/2 mouse model (14), the Q175 knock-in mouse model used in the present study is a slower-onset HD model that uses the extended CAG repeat (~179 repeats) mutation that is observed in humans (15). Motor deficits are observed at approximately 5 months in homozygotes, and they progressively decline toward hypoactivity around 8 months. Behavioral and motor deficits have a slower onset in heterozygotes (15). Reductions in cortical and striatal volumes are reported by 4 months of age in homozygotes and heterozygotes (16). The heterozygotes are more useful for

molecular analysis of the magnitude seen in this study because of the excessive atrophy seen in the homozygote brains at young age. Furthermore, homozygosity is exceedingly rare in human HD patients.

Activities for all of the enzymes of the TCA cycle and PDHC were measured. mRNA was measured in Q175 mouse cortex but not in humans because of concern about postmortem mRNA stability. Protein levels of select enzymes and enzyme complexes were determined by Western blots. Molecular analysis of human brains is often compromised by several factors, including postmortem autolysis, biological alterations caused by any drugs the patients may have been taking before the time of death, and changes induced during death. Nonetheless, human autopsy brains still provide a direct measurement in patients that died with the disease. A greater understanding of abnormalities in the TCA cycle may reveal options for further studies on therapeutic targets in HD.

MATERIALS AND METHODS

Mouse Brain Shipment, Storage and Preparation

All procedures in mice were approved by the Institutional Animal Care and Use Committee of Weill Cornell Medical College. Frozen mouse brains were received on dry ice from CRL Discovery Research Services (Kuopio, Finland). They were immediately stored at −80°C at the Burke Medical Research Institute (White Plains, NY). Unless specifically noted otherwise, all of the brains were pulverized to fine powder in liquid nitrogen and stored at −80°C until use. They were further homogenized via sonication to create lysates immediately before molecular analysis.

Studies were designed to validate enzyme stability up to 36 hours postmortem in mouse cortex before proceeding to human measurements. The selected time points were 0, 12, 24 and 36 hours postmortem. Twenty wild type male mice at 6 to 8 weeks of age were killed by an overdose of CO_2. Bodies were placed at 4°C for the indicated postmortem times (n = 5 per time point). Cortices (left and right pooled) and striata (left and right pooled) were dissected on ice and frozen at −80°C until shipment. The pooled samples were received and stored at Burke Medical Research Institute at −80°C.

The Q175 mice and the wild type litter matched controls are described in previous publications (15, 16). For the Q175 mouse cortex and striatum studies at 14 to 15 months, 48 wild type brains (16 males to 32 females) and 50 heterozygote brains (16 males to 34 females) were dissected and shipped to Burke Medical Research Institute. Between 8 and 11 striata were crushed to powder in liquid nitrogen and pooled, without mixing genotypes and genders, to yield an n = 1. The pooling process was repeated to yield a final of n = 5 per group (2 groups: heterozygote and control) for the striatal studies. Similarly, 3 cortices were crushed to powder in liquid nitrogen and pooled, without mixing genotypes and genders, to yield n = 1. This pooling process was repeated to yield a total of n = 5 per group (2 groups: heterozygote and control) for the cortical studies.

Human Brains

The use of human brains was approved by the Internal Review Boards at Columbia University and Burke Rehabilitation Hospital. The authors could not match results with the identities of any of the patients. For the human cortex studies, 14 control cortices (7 males to 7 females) and 14 HD cortices (8 males to 6 females) were received from JPV and EPS at the New York Brain Bank at Columbia University (New York, NY). Samples were all from the parietal cortex (as much as possible from Brodmann area 17). The human brains were collected at varying postmortem time points (Table 1). The subjects were initially placed in a cold room, the earliest at 5 minutes and the latest at 21 hours after time of death. The brains were frozen at varying postmortem times, ranging from 4.9 to 32.5 hours after death. All of the brains were prepared according to Protocol 1 (17). HD was diagnosed by standard criteria (18).

mRNA Measurements

Mouse brains were stored for 3 to 4 months at −80°C. Total RNA was extracted using the RNeasy Lipid Tissue Mini Kit from Qiagen (Venlo, the Netherlands). RNA concentrations and detection of potential protein impurities were measured using a NanoDrop machine (Nano Drop 1000 spectrophotometer from Thermo Scientific, Waltham, MA). The High Capacity Reverse Transcription Kit with RNase Inhibitor (Life Technologies, Grand Island, NY) was used to synthesize cDNA. Mouse primers were obtained from Life Technologies. Real Time-PCR was run using TaqMan Fast Universal PCR Master Mix, No AmpErase UNG (Life Technologies) using a 7500 Fast RT-PCR machine from Applied Biosystems (Life Technologies): 20 seconds at 95°C; 45 cycles for 3 seconds at 95°C and 30 seconds at 60°C, total volume equals 20 μl. Each target gene was measured in triplicate. *HPRT1* was selected as the endogenous control after careful establishment of consistently reproducible measurements across different samples.

Enzyme Activity Measurements

Each assay is standardized to a commercial enzyme each time the assay is run to minimize the between-run variance. Nevertheless, all of the mouse or human brain samples for a particular enzyme were run at the same time to avoid between-day variations. Although the human and mouse brains for a particular enzyme were run on different days, vast differences were found between mouse and human specific activities.

Enzyme activity measurements were made in lysates of frozen brains. All of the reagents for these assays were received from Sigma-Aldrich (St. Louis, MO).

Pyruvate dehydrogenase complex (PDHC) activity was estimated by coupling the production of acetyl-CoA to the acetylation of aminoazobenzoic acid with arylamine acetyltransferase. The reaction was measured at 460 nm at 37°C using a SpectraMax 250 plate reader (Molecular Devices, Sunnyvale, CA.) for 42 minutes (9). Arylamine acetyltransferase was purified in our laboratory using pigeon liver acetone powder (Sigma-Aldrich, L-8376) following a previously established protocol (19).

Citrate synthase (CS) activity was estimated by coupling coenzyme A to Ellman's reagent, 5, 5′ dithiobis-(2-nitrobenzoic acid). The reaction was measured using a SpectraMax 250 plate reader at 412 nm at 37°C for 15 minutes (9).

Aconitase activity is inactivated when exposed to oxidation and freeze-thaw cycles (20). Activity can be reactivated by using a mixture of sodium thiomalate (20 mM) and ferrous ammonium sulfate (4 mM) at 37°C for 30 minutes. Aconitase activity was estimated by measuring the reduction of NADP using a Gemini EM fluorescent plate reader (Molecular Devices) at 340 nm at 30°C for 30 minutes (9).

Isocitrate dehydrogenase (ICDH) activity was estimated by measuring the reduction of NADP using a Gemini EM fluorescent plate reader at 340 nm at 30°C for 15 minutes (9).

α-Ketoglutarate dehydrogenase complex (KGDHC) activity was measured using a mixture of NAD and CoA coupled with α-ketoglutaric acid; the activity was estimated by measuring the production of NADH using a Gemini EM fluorescent plate reader at 340 nm at 37°C for 30 minutes (9).

Succinyl thiokinase (STH) activity was estimated by measuring the formation of NAD using a Gemini EM fluorescent plate reader at 340 nm at 30°C for 20 minutes (9).

Succinate dehydrogenase (SDH) activity was estimated by measuring the reduction of 2,6-dichloroindophenol (DCIP) using a SpectraMax 250 plate reader at 600 nm at 37°C for 10 minutes (9).

Fumarase activity was estimated by measuring the conversion of L-malate to fumarate using a SpectraMax 250 plate reader at 250 nm at 25°C for 15 minutes (9). The reaction uniquely uses Costar acrylic 96-well flat bottom UV plates because plastic materials filter shorter wavelengths of light.

Malate dehydrogenase (MDH) activity was estimated by measuring the rate of oxidation of NADH in the presence of oxaloacetate using a Gemini EM fluorescent plate reader at 340 nm at 25° C for 25 minutes (9).

Protein Measurements

Protein levels were measured using a Bradford Coomassie brilliant blue dye-binding procedure (Bio-Rad 500-006 kit; Bio-Rad Laboratories, Hercules, C.A.) (21). Bovine serum albumin (Sigma-Aldrich) was used as the reference standard.

Western Blot Analysis

The proteins were loaded onto Novex Tris-Glycine 4%–20% gels (Life Technologies) and then transferred overnight onto nitrocellulose paper (Bio-Rad Laboratories). After blocking with Li-COR Odyssey Blocking Buffer (Li-COR Biosciences, Lincoln, NE), diluted in Tris buffered saline, primary β-actin rabbit monoclonal antibody from Cell Signaling Technology (Beverly, MA) or mouse β-actin primary polyclonal antibody (Cell Signaling 4970S), and secondary goat anti-rabbit IgG (Li-COR 926-68071) and secondary goat anti-mouse antibodies (Li-COR 926-32210) were added to detect β-actin and the protein of interest.

Antibodies from Abcam (Cambridge, UK) were: anti-SDHB (SDH) (ab14714), mitoProfile pyruvate dehydrogenase WB Antibody Cocktail (PDHC), anti-pyruvate dehydrogenase (PDH) cocktail [Abcam (ab110416) for the following proteins: 69 kDa E2, 54 kDa E3, 43.3 kDa E1α, 39.4 kDaE1β], anti-aconitase 2 (ab71440), anti-MDH2 (MDH) and anti-succinate dehydrogenase (ab14714) (28 kDa)]. The membranes were scanned using the LiCOR Odyssey instrument.

qPCR Calculation and Statistical Analysis

Real Time-PCR was performed on 5 wild type and five heterozygous Q175 mouse cortices. Target genes were measured in triplicate for each sample. Gene expression relative to the internal control *HPRT1* were calculated for each brain and then averaged for wild types and heterozygotes. The difference in average relative expression between wild types and heterozygotes was assessed for significance using a Student t-test at $p \leq 0.05$.

Enzyme Activity Calculations and Statistical Analysis

Enzyme standards from Sigma were used to establish a linear range of activity tracings before every assay (data not shown). Each sample was measured in triplicate and then averaged. Outliers were eliminated using a Q-test at 80% to 85% confidence (22). These values (mean ± SEM) were then averaged with the other samples of the same group. For the human brain studies, the difference in mean enzyme activities between HD and control brains was assessed using a Student t-test at $p \leq 0.05$. For the Q175 mouse studies, ANOVA was followed by a Student-Newman-Keuls post hoc test at $p \leq 0.05$ to compare the differences between wild type and heterozygote enzyme activities, and also the differences between cortical and striatal enzyme activities.

Calculations Related to Western Blots

For the human studies, all of the specific activities were either unchanged or increased in HD cortex compared to control. We rationalized that protein levels would be worth evaluating only if there was a difference in protein levels at the extreme levels of specific activity for the highest HD brain and lowest control brain (i.e. the most extreme cases). Thus, proteins were initially measured for the HD brain with the highest activity and the control brain with the lowest activity. If they were not different, further analyses of the samples were not undertaken. For the Q175 mouse studies, proteins were measured for all 10 cortices (5 controls and 5 heterozygotes). Membrane scans were evaluated and quantified using Odyssey 3.0 software (Li-Cor Biosciences). Band intensities were measured for the enzymes of interest and the normalizer, β-actin. The ratio of enzyme band intensity to normalized β-actin band intensity was averaged for each subject group. The differences between control and HD human brains or wild type and heterozygote brains for the mice were compared. Significance was assessed at $p \leq 0.05$ using a Student t-test.

RESULTS

Q175 Mouse Brain Studies

The activities of all of the TCA cycle enzymes and PDHC (Fig. 1) were determined concurrently in the cortex (Fig. 2A) and striatum (Fig. 2B) of Q175 heterozygous and wild

type mice at 14 to 15 months. These measurements allow for the comparison of activities within each brain region as well as between brain regions. MDH and fumarase had the highest activities in both brain regions. STH was intermediate whereas SDH and KGDHC were the lowest.

There were clear differences in enzyme activities between wild type and heterozygous mice in cortex but not in striatum. Increased activities in heterozygous cortex compared to wild type cortex were measured in PDHC (+12%), aconitase (+32%) and SDH (+23%) (Fig. 2A). None of the variables were different in the striatum between wild types and heterozygotes (Fig. 2B). There were non-significant differences not exceeding more than 10% between the sexes (data not shown). A limited number of Q175 cortex samples were also examined at 9 months, but no differences occurred between controls and heterozygotes for any of the variables (data not shown).

Comparisons of striatum and cortex revealed further differences between wild types and heterozygotes. In the wild types, CS activity was 22% significantly lower in striatum than in cortex. On the other hand, in heterozygotes, KGDHC (+9%) and SDH (+16%) activities were significantly higher in striatum than in cortex, whereas STH (−18%) activity was significantly lower in striatum than in cortex (Fig. 2A, B).

The levels of select proteins in the cortex of wild type and Q175 heterozygotes were compared by Western blot. The E3bp subunit of the PDH complex was elevated by 39% in heterozygotes compared to wild types in cortex while subunits E1p and E2p were unchanged (Fig. 3A). No differences were found between wild types and heterozygotes in aconitase (Fig. 3B) or SDH (Fig. 3C) protein levels in cortex. Quantification of these Western blots, normalized to β-actin, is provided (Fig. 3D).

mRNA levels were compared in the cortices of Q175 wild type and heterozygous mice. Wild type gene expression levels relative to the internal control, *HPRT1*, are listed for the genes relevant to transketolase, PDHC and the enzymes of the TCA cycle (Fig. 1). The threshold detection level for PDHA2 was below an accurate range of detection. The remaining genes were in an acceptable range for qPCR analysis. The genes coding for MDH exhibited the highest mRNA expression out of all of the genes that were measured. Similarly, MDH enzyme activity eclipsed that of all other TCA cycle enzymes, and by as much as 100-fold in comparison to SDH activity. In contrast, fumarase had the second highest activity, but the mRNA was lower than those for other TCA cycle enzymes that had lower activities such as KGDHC and SDH.

Changes in mRNA expression were calculated between wild types and heterozygotes. Although many differences were significant, only those greater than 20% are presented (Fig. 3E). mRNA expression levels for transketolase (TKT) (+27%), isocitrate dehydrogenase 1 (IDH1) (+57%) and succinyl-CoA ligase α subunit (SUCLG1) (+83%) were increased while pyruvate dehydrogenase phosphatase (PDP1) was decreased (−40%) in heterozygote cortex compared to wild type cortex.

Comparison of Brains from HD Patients and Controls

The proteins and activities related to the TCA cycle were also tested in human brain samples. Autopsy brains are much more variable because of differences of drug therapies, cause of death, the postmortem intervals and time before the brain was frozen. The postmortem interval was modeled in wild type mouse cortex up to 36 hours after time of death. No significant differences were found in any of the nine enzymes of interest (Fig. 4A). None of the human brains exceeded the 36-hour limit that was tested in mice.

Most of the enzyme activities were similar between control and HD cortex (Fig. 4B). SDH activity was significantly higher in HD cortex compared to control human brains by 35% ($p \leq 0.05$). PDHC was reduced by 10% to 15% but the differences were not significant.

Specific activities were lower in control human cortex compared to wild type mouse cortex at the 0 hour time point from the postmortem studies for most of the enzymes (Fig. 5). Only ICDH activity was about the same in both humans and mice. As a percentage of mouse cortex enzyme activities, human PDHC (44%), CS (65%), aconitase (16%), KGDHC (18%), STH (12%), SDH (29%), fumarase (21%) and MDH (75%) activities were only fractions of the levels seen in mice. These findings suggest that mitochondrial metabolic capacity is significantly lower in humans than in mice.

Western blot was used to compare SDH protein levels from the control brain with the lowest activity and the HD brain with the highest (Fig. 6A). No difference was found in SDH protein levels between the control and HD cortex (Fig. 6B). Because even the extremes did not show differences, the remaining samples were not examined. MDH protein was also measured by Western blot in the brains, but no differences were revealed (data not shown).

mRNA expression levels were not measured in the human brains. KGDHC mRNAs (*OGDH, DLD, DLST*) were measured in wild type mice to test for postmortem mRNA stability. The results were varied and unstable up to 36 hours postmortem, especially for *DLD* and *DLST* expression levels (Fig. 7). Thus, mRNA levels would likely be unstable in the human brains as well.

DISCUSSION

The goals of this study were to test whether the TCA cycle is altered in brains from HD patients at autopsy or in the Q175 mouse model of HD. Although a large number of studies have examined the electron transport chain in HD, none have examined the TCA cycle in its entirety. Furthermore, none of these measurements has been made in Q175 mice. Specific activities are considerably lower in control human cortex compared to wild type mouse cortex. Only ICDH activity was about the same in both humans and mice. The remaining TCA cycle enzyme activities in humans are only a fraction of those seen in mice. This suggests that mitochondrial metabolic capacity is significantly lower in humans than in mice. This difference must be considered when extrapolating from mouse models to humans.

Many of the results were unexpected. Increases in enzyme activities in the cortex but not in the striatum of Q175 heterozygotes compared to wild types was surprising because the striatum is generally regarded as the more sensitive brain region in models of HD as well as in HD. Several enzyme and mRNA measurements, including those for ICDH, STH and MDH, were measured in HD for the first time. The increases in PDHC, aconitase and SDH activities in cortices from Q175 heterozygotes differ from what the HD literature would predict. All measured activities in human cortex from the current study and a summary of reported measurements in other regions of HD human brains are listed in Table 2.

In studies on the molecular basis of neurodegenerative diseases, any analyses and conclusions must be considered in light of compromises due to excessive neurodegeneration or degradation of the molecules of interest either before or after death. Although the striatum is the most sensitive and perhaps most revealing brain region, it is often so severely degenerated by the time an HD patient dies that measurements have little meaning. This difficulty is hard to overcome in humans because the number of patients who die at early stages in the disease from other causes is small. Time course studies in mice can obviate this problem because postmortem changes in brain tissue can be modeled in mice. We evaluated enzyme activities in mouse cortex from 0 to 36 hours after death to determine whether accurate measures of activity could be obtained in human brains with long postmortem times. In confirmation and extension of previous studies (7), the postmortem analysis in mice suggests the activities of the enzymes are stable for at least 36 hours after time of death. However, fold changes in gene expression were highly variable over the postmortem time course measurements for the 3 genes that encode for the KGDH complex, particularly for the genes DLD and DLST. This variability suggested that mRNA expression in human brains would also be unstable; thus, the tissues were not suitable for RT-PCR. Therefore, we did not evaluate mRNA levels in the human brain samples.

Increases in mRNA levels in cortex of the Q175 mice are consistent with activation of the TCA cycle and the pentose shunt. Significant increases were found in mRNAs for IDH1 and SUCLG1 in Q175 mouse cortex compared to cortex from wild type mice. mRNA for transketolase, a rate controlling step in the pentose shunt, was also increased.

PDHC, which catalyzes the entry step into the TCA cycle, plays a key role in energy metabolism and consequently in the pathophysiology of HD. Activity levels decrease in the putamen, caudate nucleus and hippocampus of brains from HD patients compared to controls, but not in cortex (10, 23). Additionally, activation of PDHC is very beneficial in R6/2 mice (24). The reduction in PDHC activity in autopsy HD brains (−25%; non-significant) in the current study is consistent with the literature (Table 2). However, PDHC activities in the cortex of Q175 heterozygotes were higher than in wild type cortex. The mouse brains were not subjected to typical compromises and drug effects that are seen in autopsy human brains. Additionally, the reduction in striatal volume by 14 to 15 months of age or even earlier in these heterozygotes indicates that there is indeed an HD phenotype (16). Therefore, hypotheses about the role of PDHC in HD must account for this reported increase in PDHC activity.

The decrease in mRNA for one of 2 known isoforms of PDP1 emphasizes the importance of PDHC alterations in Q175 mice. PDHC is continuously regulated by phosphorylation and dephosphorylation (25). The phosphatase coded for by *PDP1* regulates dephosphorylation, or activation, of PDHC (26). mRNA levels do not predict protein levels, but the fact that it was 1 of only 4 mRNAs that were altered is indicative of the sensitivity of pyruvate metabolism to HD pathology. Further studies on PDHC metabolic regulation may reveal new understandings of the role of the enzyme complex in HD.

Aconitase catalyzes the conversion of citrate to isocitrate. The literature suggests aconitase activity is depressed in cortex and striatum from patients who died with HD (12), and in the cortex and striatum of R6/2 mice (27). Our findings in human HD brains, although not significant, agree with former studies of aconitase activity in human HD brains. However, aconitase activity was significantly elevated in the cortex of Q175 compared to wild type mice at 14 to 15 months, although it was unaffected in Q175 heterozygote striatum compared to wild type striatum. Studies of human lymphoblasts from patients with HD suggest that the reported decrease in aconitase activity may be secondary to the pathology of the disease including oxidative stress (unpublished data). Once again, this seemingly contradictory finding may be attributed to the greater stability of mouse tissue studies compared to those of autopsy human brains.

Studies in humans and mice link decreases in SDH, also known as complex II of the electron transport chain, to striatal vulnerabilities in HD (13, 23, 28, 29). Inhibiting complex II with 3-nitroproprionic acid or malonate in rats and primates leads to increased striatal degeneration that closely mimics the pathology seen in HD (28, 29). Furthermore, SDH activity, which is unchanged in HD cortex, is decreased in the caudate nucleus of HD brains compared to controls (23, 30, 31). This study reports for the first time an increase in SDH activity compared to controls in both Q175 heterozygous mouse cortex (+23%) and in cortex from HD patients (+35%). The increase in activity suggests that complex II is under intense stress in HD. However, the fact that SDH protein measured by Western blots did not change in either mice or humans suggests that post-translational modifications may be important.

While the increase in SDH in HD is similar to other diseases such as AD and schizophrenia, the other changes vary from what is seen in those diseases. The increase in SDH in brains from Q175 mice and humans with HD is similar to the increase we observed in brains from AD (8) and schizophrenic (7) patients. In AD, PDHC, ICDH and KGDHC activities decrease while SDH and MDH activities increase (8). In schizophrenia, aconitase and STH activities decrease while SDH and MDH activities increase compared to controls (7). Reportedly, in HD, CS (12, 32) and KGDHC (11), activities decrease in the putamen. Neither of these changes was observed in human cortex in this study. Additionally, the lack of change in fumarate hydratase activity agrees with other reports in cortex, caudate nucleus, putamen and hippocampus of HD brains (10). Overall, enzyme activities were normal in the HD brains compared to controls except for SDH. Enzyme activity measurements demonstrate that increased SDH activity is common to many diseases. Inhibiting SDH leads to an HD phenotype; therefore, this increase may be a protective mechanism.

Conclusion

Changes in metabolic enzyme activities are well documented in several neurological disorders including HD. This is the first study in which all of the enzymes of the TCA cycle were evaluated concurrently in either HD brains or any mouse models of HD. Measurements in both mouse and human support the importance and consistency of an increase in SDH. The mouse studies suggest an increase, not a decrease, in TCA cycle activity.

ACKNOWLEDGMENT

We thank Jukka Puoliväli from CRL Discovery Research Services (Kuopio, Finland) for providing Q175 mouse tissues.

Funding was provided by CHDI Foundation, NIH PP-AG14930, and the Burke Medical Research Institute.

REFERENCES

1. Vonsattel JP, DiFiglia M. Huntington disease. J Neuropath Exper Neurol. 1998; 57:369–384. [PubMed: 9596408]
2. MacDonald ME, Ambrose CM, Duyao MP, et al. A novel gene containing a trinucleotide repeat that is expanded and unstable on Huntington's disease chromosomes. Cell. 1993; 72:971–983. [PubMed: 8458085]
3. Hazeki N, Nakamura K, Goto J, et al. Rapid aggregate formation of the huntingtin N-terminal fragment carrying an expanded polyglutamine tract. Biochem Biophys Res Comm. 1999; 256:361–366. [PubMed: 10079189]
4. Kuhl DE, Markham CH, Metter EJ, et al. Local cerebral glucose utilization in symptomatic and presymptomatic Huntington's disease. Res Publ Assoc Res Nerv Ment Dis. 1985; 63:199–209. [PubMed: 3161165]
5. Kuhl DE, Metter EJ, Riege WH, et al. Patterns of cerebral glucose utilization in Parkinson's disease and Huntington's disease. Ann Neurol. 1984; 15:119–125. [PubMed: 6703651]
6. Kuhl DE, Phelps ME, Markham CH, et al. Cerebral metabolism and atrophy in huntington's disease determined by 18FDG and computed tomographic scan. Ann Neurol. 1982; 12:425–434. [PubMed: 6217782]
7. Bubber P, Hartounian V, Gibson GE, et al. Abnormalities in the tricarboxylic acid (TCA) cycle in the brains of schizophrenia patients. Eur Neuropsychopharmacol. 2011; 21:254–260. [PubMed: 21123035]
8. Bubber P, Haroutunian V, Fisch G, et al. Mitochondrial abnormalities in Alzheimer brain: mechanistic implications. Ann Neurol. 2005; 57:695–703. [PubMed: 15852400]
9. Bubber P, Ke ZJ, Gibson GE. Tricarboxylic acid cycle enzymes following thiamine deficiency. Neurochem Intl. 2004; 45:1021–1028.
10. Sorbi S, Bird ED, Blass JP. Decreased pyruvate dehydrogenase complex activity in Huntington and Alzheimer brain. Ann Neurol. 1983; 13:72–78. [PubMed: 6219611]
11. Klivenyi P, Starkov AA, Calingasan NY, et al. Mice deficient in dihydrolipoamide dehydrogenase show increased vulnerability to MPTP, malonate and 3-nitropropionic acid neurotoxicity. J Neurochem. 88; 1352:60.
12. Tabrizi SJ, Cleeter MWJ, Xuereb J, et al. Biochemical abnormalities and rxcitotoxicity in Huntington's disease brain. Ann Neurol. 1999; 45:25–32. [PubMed: 9894873]
13. Benchoua A, Trioulier Y, Zala D, et al. Involvement of mitochondrial complex II defects in neuronal death produced by N-terminus fragment of mutated huntingtin. Mol Biol Cell. 2006; 17:1652–1663. [PubMed: 16452635]
14. Mangiarini L, Sathasivam K, Seller M, et al. Exon 1 of the HD gene with an expanded CAG repeat is sufficient to cause a progressive neurological phenotype in transgenic mice. Cell. 1996; 87:493–506. [PubMed: 8898202]

15. Menalled LB, Kudwa AE, Miller S, et al. Comprehensive behavioral and molecular characterization of a new knock-in mouse model of Huntington's Disease: zQ175. PLoS ONE. 2012; 7:e49838. [PubMed: 23284626]
16. Heikkinen T, Lehtim‰ki K, Vartiainen N, et al. Characterization of neurophysiological and behavioral changes, MRI brain volumetry and 1H MRS in zQ175 knock-in mouse model of Huntington's Disease. PLoS ONE. 2012; 7:e50717. [PubMed: 23284644]
17. Vonsattel JP, Del Amaya MP, Keller CE. Twenty-first century brain banking. Processing brains for research: the Columbia University methods. Acta Neuropath. 2008; 115:509–532. [PubMed: 17985145]
18. Vonsattel JP, Myers RH, Stevens TJ, et al. Neuropathological classification of Huntington's disease. J Neuropathol Exp Neurol. 1985; 44:559–577. [PubMed: 2932539]
19. Ksiezak-Reding H, Blass JP, Gibson GE. Studies on the pyruvate dehydrogenase complex in brain with the arylamine acetyltransferase-coupled assay. J Neurochem. 1982; 38:1627–1636. [PubMed: 7077331]
20. Kennedy MC, Emptage MH, Dreyer J-L, et al. The role of iron in the activation-inactivation of aconitase. J Biol Chem. 1983; 258:11098–11105. [PubMed: 6309829]
21. Bradford M. A rapid and sensitive method for the quantitation of microgram quantities of protein utilizing the principle of protein-dye binding. Anal Biochem. 1976; 72:248–254. [PubMed: 942051]
22. Dean RB, Dixon WJ. Simplified Statistics for Small Numbers of Observations. Anal Chem. 1950; 23:636–638.
23. Butterworth J, Yates CM, Reynolds GP. Distribution of phosphate-activated glutaminase, succinic dehydrogenase, pyruvate dehydrogenase and γ-glutamyl transpeptidase in postmortem brain from Huntington's disease and agonal cases. J Neurol Sci. 1985; 67:161–171. [PubMed: 2858515]
24. Andreassen OA, Ferrante RJ, Huang H-M, et al. Dichloroacetate exerts therapeutic effects in transgenic mouse models of Huntington's disease. Ann Neurol. 2001; 50:112–116. [PubMed: 11456300]
25. Holness MJ, Sugden MC. Regulation of pyruvate dehydrogenase complex activity by reversible phosphorylation. Biochem Soc Trans. 2003; 31:1963–2003.
26. Kolobova E, Tuganova A, Boulatnikov I, et al. Regulation of pyruvate dehydrogenase activity through phosphorylation at multiple sites. Biochem J. 2001:69–77. [PubMed: 11485553]
27. Tabrizi SJ, Workman J, Hart PE, et al. Mitochondrial dysfunction and free radical damage in the Huntington R6/2 transgenic mouse. Ann Neurol. 2001; 47:80–86. [PubMed: 10632104]
28. Beal MF, Brouillet E, Jenkins BG, et al. Neurochemical and histologic characterization of striatal excitotoxic lesions produced by the mitochondrial toxin 3-nitropropionic acid. J Neurosci. 1993; 13:4181–4192. [PubMed: 7692009]
29. Brouillet E, Hantraye P, Ferrante RJ, et al. Chronic mitochondrial energy impairment produces selective striatal degeneration and abnormal choreiform movements in primates. Proc Natl Acad Sci USA. 1995; 92:7105–7109. [PubMed: 7624378]
30. Butterworth J, Yates CM, Simpson J. Phosphate-activated glutaminase in relation to Huntington's Disease and agonal state. J Neurochem. 1983; 41:440–447. [PubMed: 6223989]
31. Gu M, Gash MT, Mann VM, et al. Mitochondrial defect in Huntington's disease caudate nucleus. Ann Neurol. 1996; 39:385–389. [PubMed: 8602759]
32. Browne SE, Bowling AC, Macgarvey U, et al. Oxidative damage and metabolic dysfunction in Huntington's disease: selective vulnerability of the basal ganglia. Ann Neurol. 1997; 41:646–653. [PubMed: 9153527]

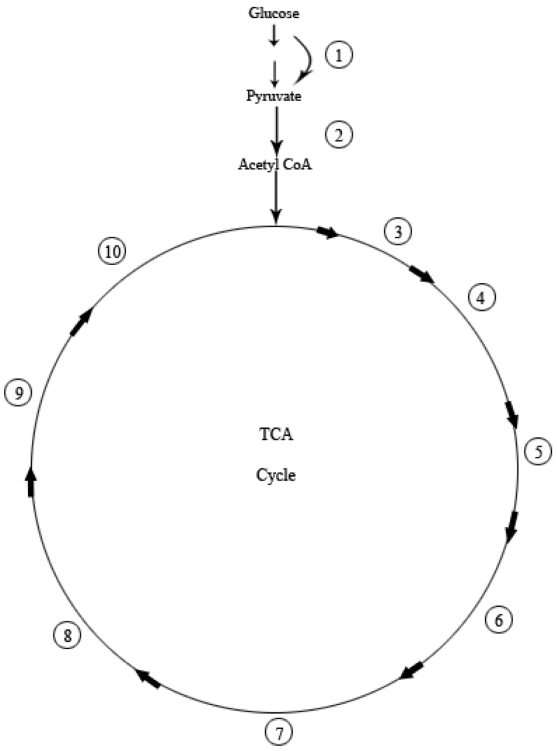

Enzyme	Gene	Control Mouse Gene Expression Relative to HPRT1
1. Transketolase	TKT	0.755 ± 0.042
2. Pyruvate Dehydrogenase Complex (PDHC)	DLD	0.792 ± 0.032
	DLAT	0.501 ± 0.015
	PDHX	0.238 ± 0.010
	PDHB	0.487 ± 0.009
	PDHA2	0.000284 ± 0.00006
	PDHA1	0.985 ± 0.032
	PDK2	0.934 ± 0.031
	PDK4	0.761 ± 0.054
	PDP1	0.907 ± 0.117
3. Citrate Synthase (CS)	CS	0.480 ± 0.009
4. Aconitase	ACO2	0.933 ± 0.022
5. Isocitrate Dehydrogenase (ICDH)	IDH1	0.244 ± 0.006
	IDH2	0.120 ± 0.005
	IDH3G	1.762 ± 0.043
	IDH3B	0.770 ± 0.031
	IDH3A	1.773 ± 0.043
6. α-Ketoglutarate Dehydrogenase Complex (KGDHC)	DLD	0.792 ± 0.032
	DLST	0.479 ± 0.018
	OGDH	0.871 ± 0.035
7. Succinyl Thiokinase (STH)	SUCLG2	0.116 ± 0.004
	SUCLG1	0.454 ± 0.021
	SUCLA2	0.500 ± 0.009
8. Succinate Dehydrogenase (SDH)	SDHD	0.472 ± 0.020
	SDHC	0.838 ± 0.041
	SDHB	0.524 ± 0.026
	SDHA	1.914 ± 0.052
9. Fumarase	FH	0.497 ± 0.015
10. Malate Dehydrogenase (MDH)	MDH1	3.956 ± 0.077
	MDH2	3.365 ± 0.171

Figure 1.

Genes associated with the enzymes of the tricarboxlyic acid (TCA) cycle, pyruvate dehydrogenase complex (PDHC) and transketolase. The 29 genes listed were selected based on their roles in the 9 enzymes that were examined. Most of these genes either code for subunits of the enzymes or for proteins that play integral roles in their functions (e.g. the kinases for PDHC). Gene expressions relative to *HPRT1* ± SE are listed for wild type mouse cortex (n = 5).

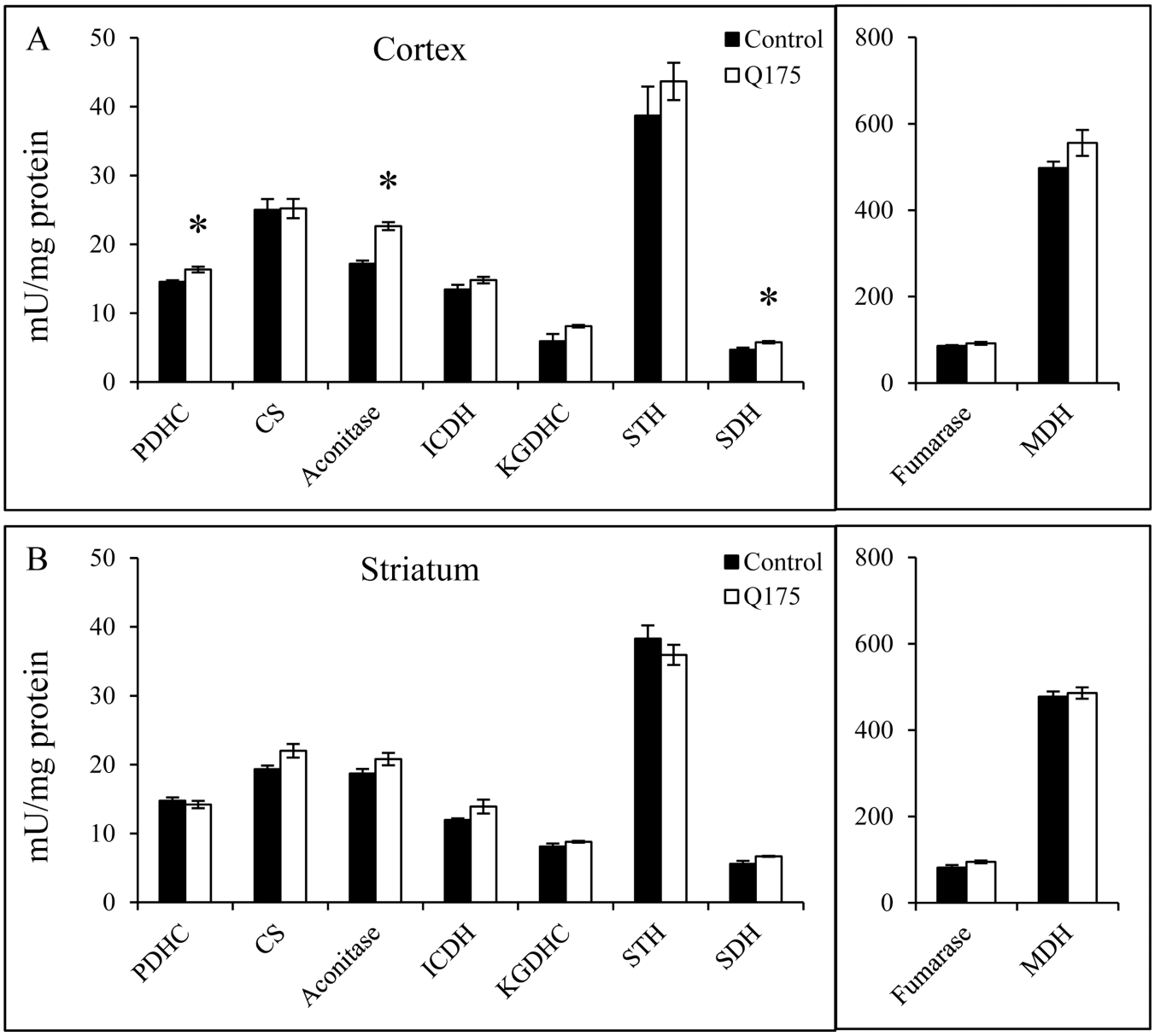

Figure 2.

Enzyme activity measurements in Q175 mice at 14 to 15 months of age. (**A**) Specific activities were measured in cortex for the same enzymes in control and Q175 mice at 14 to 15 months of age. Three cortices were pooled to create an n of 1. N = 5 for each enzyme. (**B**) Specific activities were measured in striatum for pyruvate dehydrogenase complex (PDHC) and the eight enzymes of the tricarboxlyic acid (TCA) cycle in control and Q175 mice at 14 to 15 months of age. Eight to 11 striata were pooled to create an n of 1. N = 5 for each enzyme. Significance was assessed using a Student t-test at $p \leq 0.05$. *Denotes a significant difference between control and Q175. CS, citrate synthase; ICDH, isocitrate dehydrogenase; KGDHC, α-ketoglutarate dehydrogenase complex, STH, succinyl thiokinase; SDH, succinate dehydrogenase; MDH, malate dehydrogenase.

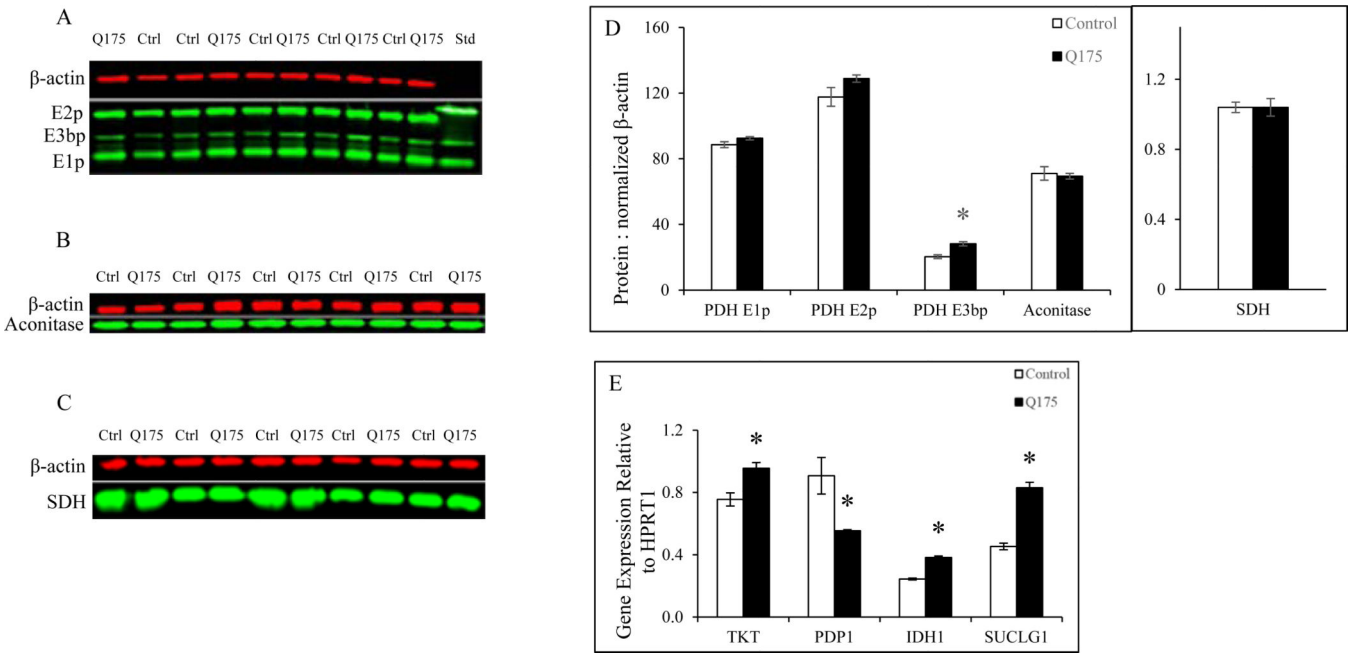

Figure 3.

Protein and mRNA levels in mouse cortex. (**A–C**) Protein levels were measured for the selected enzymes that showed changes in activity in Q175 cortex compared to control cortex. Western blots are shown for pyruvate dehydrogenase complex (PDHC) subunits E1p, E2p, E3bp (**A**), aconitase (**B**) and succinate dehydrogenase (SDH) (**C**). Five control and 5 Q175 mouse cortices were measured using 15 μg of brain lysate per well. (**D**) The intensities of the β-actin bands (red) were normalized to the highest intensity. Then the intensities of the enzyme bands (green) were divided by the normalized intensities of the β-actin bands for each respective measurement. This final ratio was calculated for each brain. The final ratios for the 5 brains in each group were averaged and compared using a Student t-test at $p \leq 0.05$. (**E**) Gene expression relative to *HPRT1* was measured by RT-PCR in 5 control and 5 Q175 mouse cortices at 14 to 15 months of age for the 29 genes listed in Figure 1. Shown are the significant changes over 20% in either direction at $p \leq 0.05$ using Student t-test. TKT, transketolase; PDP1 pyruvate dehydrogenase phosphatase; IDH1, isocitrate dehydrogenase 1; SUCLG1, succinyl-CoA ligase α subunit.

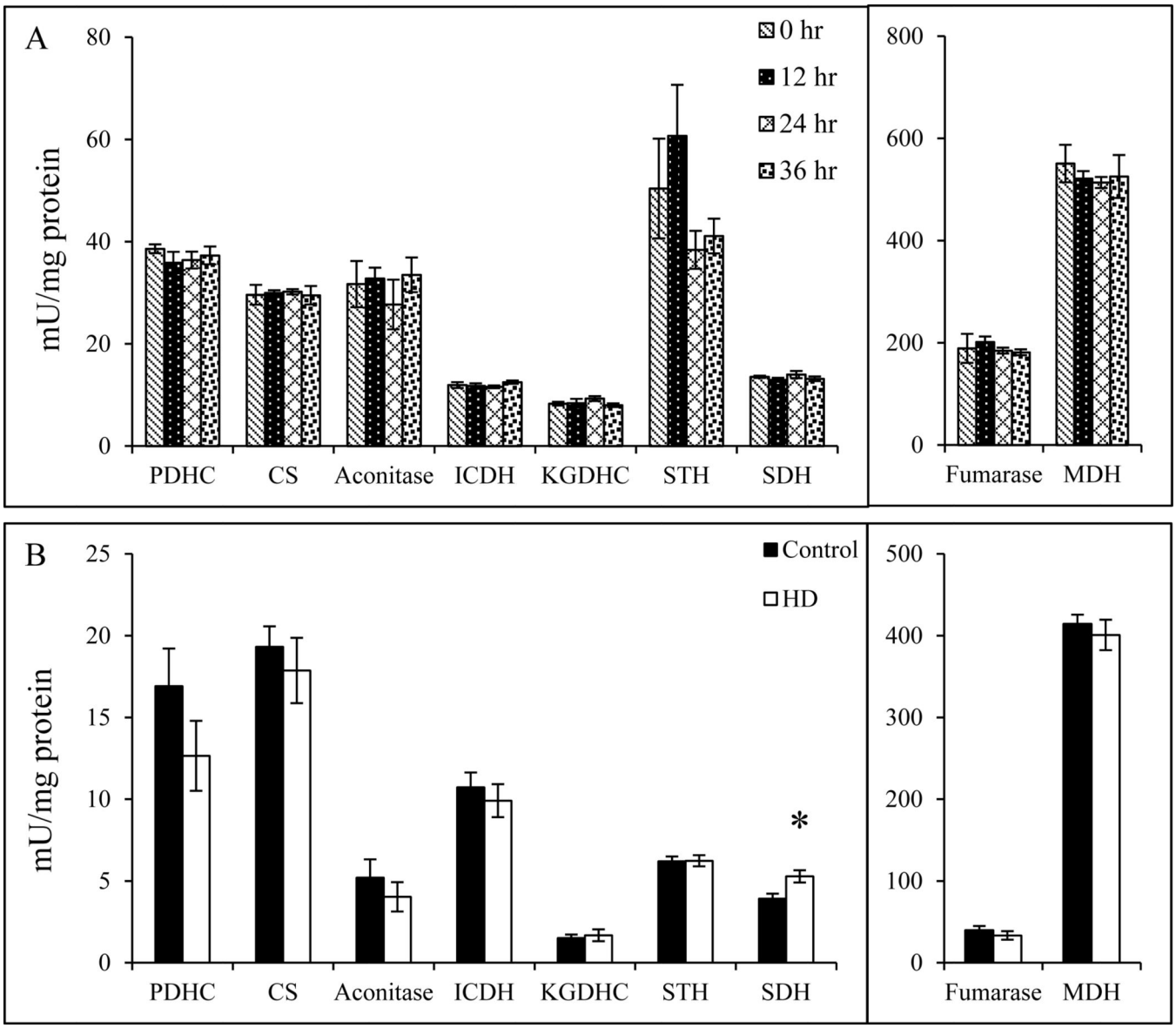

Figure 4.

Postmortem stability in wild type mouse cortex establishes validity for further measurements in Huntington disease brains. (**A**) Postmortem stability in wild type mouse cortex was established by measuring enzyme activities for all 9 enzymes of interest at 0, 12, 24, and 36 hours after death by CO_2 asphyxiation. The mice were stored at 4°C until the indicated time points. No significant changes were found in any of the 9 enzymes of interest, indicating that these enzymes are stable for at least 36 hours postmortem in wild type mouse cortex. (**B**) Specific activities for the pyruvate dehydrogenase complex (PDHC) and eight enzymes of the tricarboxlyic acid (TCA) cycle in control and Huntington disease (HD) brains were measured. n = 14 for each enzyme except for PDHC (control, n = 12; HD, n = 8), isocitrate dehydrogenase (ICDH) (control, n = 14; HD, n = 13), α-ketoglutarate dehydrogenase complex (KGDHC) (control, n = 12; HD, n = 9) and fumarase (control, n = 11; HD n = 11). Significance was assessed using a Student t-test at $p \leq 0.05$. CS, citrate synthase; ICDH,

isocitrate dehydrogenase; STH, succinyl thiokinase; SDH, succinate dehydrogenase; MCH, malate dehydrogenase.

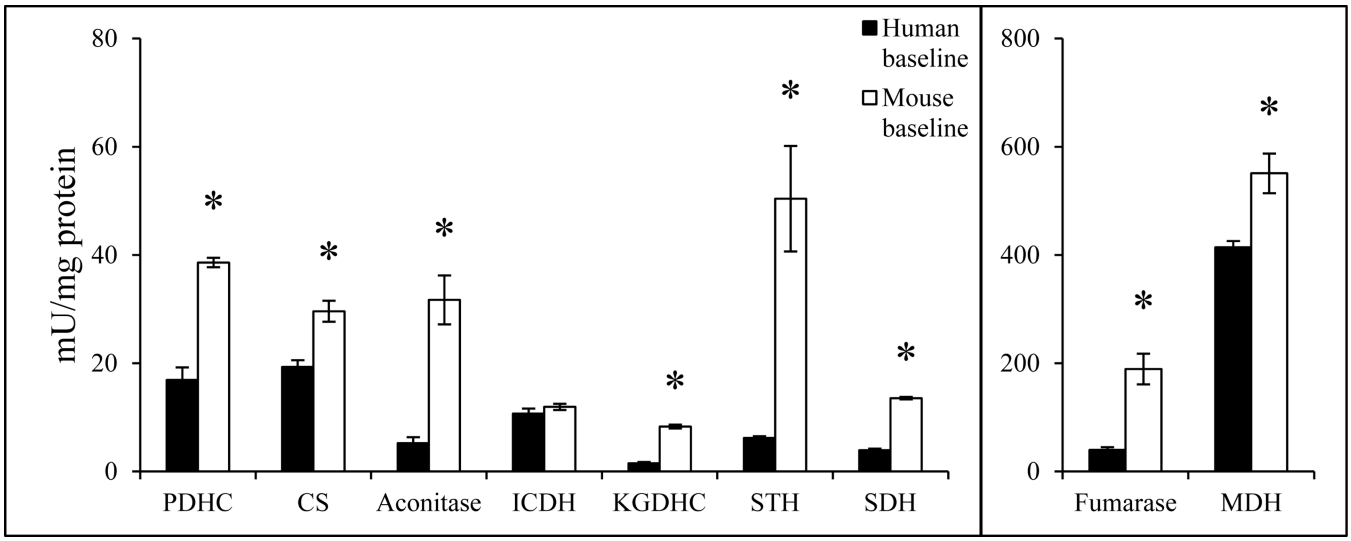

Figure 5.

Comparison of enzyme specific activities in mouse brain and human cortex. Specific activities of the nine measured enzymes in control human cortex from Figure 4B are shown alongside the same measurements in wild type mouse cortex at 0 hours from Fig. 4A. n values were the same as indicated in Figure 4A and 4B. All activities except for isocitrate dehydrogenase (ICDH) were lower in human cortex than in mouse cortex at $p \leq 0.05$ using a Student t-test. CS, citrate synthase; KGDHC, α-ketoglutarate dehydrogenase complex; STH, succinyl thiokinase; SDH, succinate dehydrogenase; MCH, malate dehydrogenase.

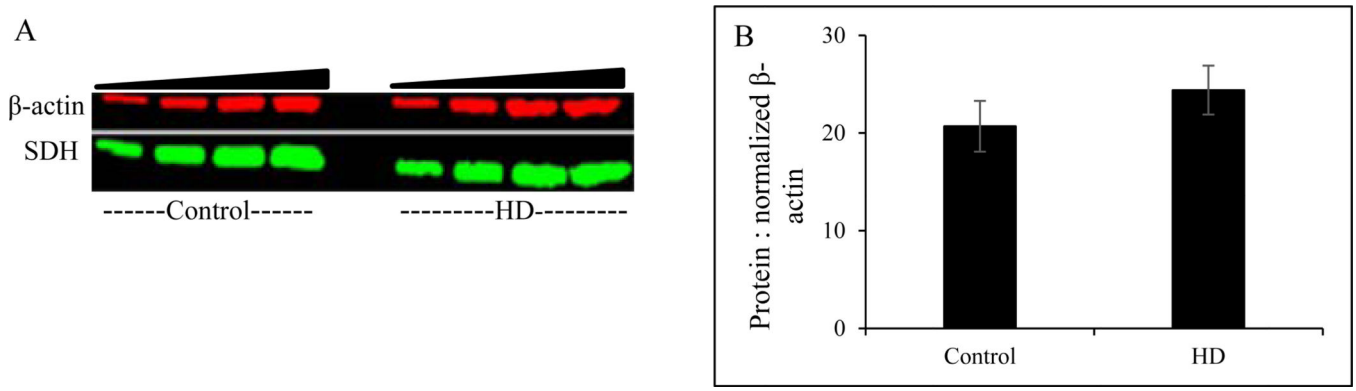

Figure 6.

Human cortex succinate dehydrogenase (SDH) Western blot. (**A**) Western blot for the control cortex with the lowest SDH specific activity and the Huntington disease (HD) cortex with the highest SDH specific activity, each measured at 4 different concentrations. Concentrations increase along the indicated gradient from left to right for control and HD (2.5 μg, 5 μg, 7.5 μg and 10 μg). (**B**) The intensities of the β-actin bands (red) were normalized to the highest intensity. Then the intensities of the SDH bands (green) were divided by the normalized intensities of the β-actin bands for each respective measurement. Differences were assessed by comparing the ratio of enzyme to normalized β-actin for each brain. The results of the four lysate concentrations were averaged together and compared between control and HD brains. No differences were found at $p \leq 0.05$ using a Student t-test.

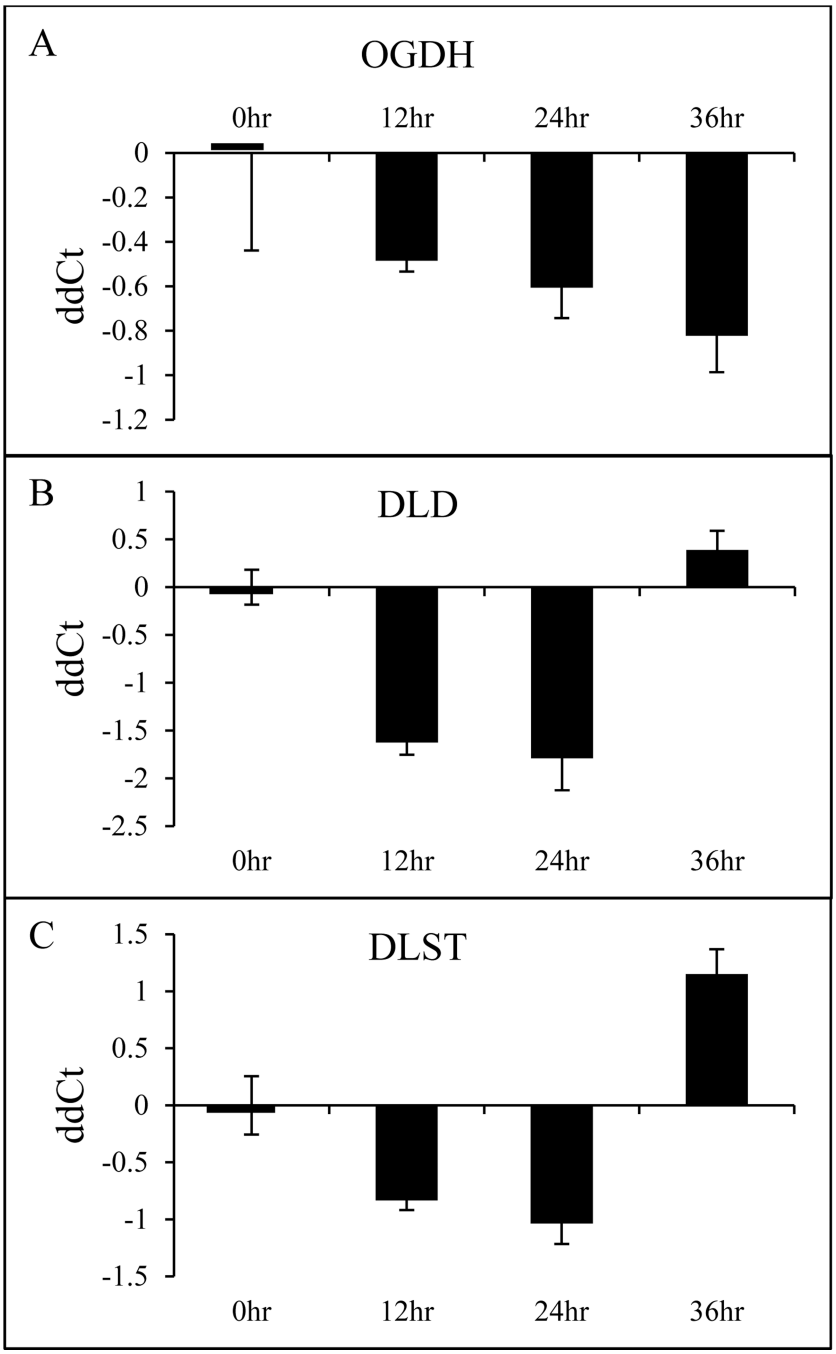

Figure 7.

mRNA changes in mouse cortex at several postmortem time points were highly variable. (**A–C**) mRNA expression was measured by RT-PCR for *OGDH* (**A**), *DLD* (**B**) and *DLST* (C), the three genes that code for the α-ketoglutarate dehydrogenase complex (KGDH) complex (n = 5 per time point). ddCt values are reported relative to the endogenous control *HPRT1*. The measured levels were too variable to justify meaningful measurements in the human autopsy brain samples.

Table 1

Characteristics of Control and Huntington Disease Patients

	Gender (Number M, F)	Age (years)[a]	Cold PMI (min)[a]	Frozen PMI (min)[a]	pH[a]	CAG Repeat[a,b]	Number at each HD grade, (i.e. 1/4, 2/4, 3/4)[c]
Control	7, 7	68.6 ± 11.8	452 ± 375	815 ± 534	6.6 ± 0.06		
HD	8, 6	67.9 ± 12.3	329 ± 277	832 ± 552	6.6 ± 0.08	43 ± 2.04 18 ± 2.10	1, 7, 6

Control and Huntington disease (HD) patient brains were matched based on gender, age, cold postmortem interval (PMI), and frozen PMI. Cold PMI is defined as the time lapse between time of death and when the body or brain is put in a cold room between 5°–10°C. Frozen PMI is calculated as the time lapse between time of death and the time that the brain is processed plus one hour (to account for harvesting and freezing time).

[a] Mean ± SE.

[b] CAG repeats for both alleles are presented for the HD patients.

[c] Number of patients at each HD grade (18).

M, male; F, female; HD, Huntington disease; min, minutes

Table 2

Tricarboxlyic Acid Enzyme and Electron Transport Chain Complex Activity Changes in Huntington Disease and Control Brains

Enzyme	Change in cortex (our lab)	Change in cortex (literature)	Change in caudate nucleus (literature)	Change in putamen (literature)	Change in hippocampus (literature)	Change in cerebellum (literature)
PDHC	−25% (not sig)	−20% (not sig) (23)	−60% (9) −70% (23)	−50% (9)	−34% (9)	
CS	No change	−27% (11) No change (31)	No change (30) No change (31)	−41% (11) −43% (31)		+42% (30)
Aconitase	−23% (not sig)	−48% (11)	−92% (11)	−73% (11)		No change (11)
ICDH[b]	No change					
KGDHC	No change			[c]decreased (10)		
STH[b]	No change					
SDH	+35%[a]	No change (23) No change (29)	−78% (23) −53% (30) −51% (29)			
FH	No change	No change (9)	No change (9)	No change (9)	No change (9)	
MDH[b]	No change					
Complex I		No change (31)	No change (30) No change (31)	No change (31)		No change (31) +35% (31)
Complex II/III		−27% (not sig) (11) −19% frontal (31)	−57% (30) −32% (31) −77% (32)	−60% (11) −71% (31)		+12% (not sig) (11) +39% (31)
Complex III			−59% (30)			
Complex IV		No change (32)	−38% (29) No change (31) −39% (not sig)(2)	−66% (31)		No change (31)

[a] $p \leq 0.05$ using Student t-test.

[b] First time these enzymes are measured in HD brains to our knowledge.

[c] Result is part of an unpublished preliminary study.

PDHC, pyruvate dehydrogenase complex; CS, citrate synthase; FH, fumarate hydratase; ICDH, isocitrate dehydrogenase; KGDHC, α-ketoglutarate dehydrogenase complex; MDH, malate dehydrogenase; SDH, succinic dehydrogenase; STH, succinyl thiokinase.